

# Folding and self-assembling with $\beta$ -oligomers based on (1*R*,2*S*)-2-aminocyclobutane-1-carboxylic acid†

Elisabeth Torres,<sup>a</sup> Esther Gorrea,<sup>a</sup> Kepa K. Burusco,<sup>a</sup> Eric Da Silva,<sup>a</sup> Pau Nolis,<sup>b</sup> Federico Rúa,<sup>a</sup> Stéphanie Boussert,<sup>c</sup> Ismael Díez-Pérez,<sup>d</sup> Samantha Dannenberg,<sup>a</sup> Sandra Izquierdo,<sup>a</sup> Ernest Giralt,<sup>c,e</sup> Carlos Jaime,<sup>a</sup> Vicenç Branchadell<sup>a</sup> and Rosa M. Ortuño<sup>\*a</sup>

Received 10th September 2009, Accepted 19th October 2009

First published as an Advance Article on the web 3rd December 2009

DOI: 10.1039/b918755c

Improved methodologies are provided to synthesize (1*R*,2*S*)-2-aminocyclobutane-1-carboxylic acid derivatives and their incorporation into  $\beta$ -peptides of 2–8 residues bearing different *N*-protecting groups. The conformational analysis of these oligomers has been carried out by using experimental techniques along with theoretical calculations. This study shows that these oligomers adopt preferentially a strand-type conformation in solution induced by the formation of intra-residue six-membered hydrogen-bonded rings, affording *cis*-fused [4.2.0]octane structural units that confer high rigidity on these  $\beta$ -peptides. Moreover, all of them are prone to self-assemble producing nano-sized fibres, as evidenced by TEM, AFM and SPFM, and, in some instances, they also form gels. These techniques and molecular modelling allowed us to suggest an aggregation model for the assembly structures in which a parallel molecular-arrangement is preferred and the conformation is similar to that observed in solution. According to this model, both hydrogen-bonding and hydrophobic interactions would account for formation of the assemblies.

## Introduction

The use of unnatural peptides in molecular architecture presents enormous possibilities for the preparation of new chiral materials with determined properties because these products can adopt well defined secondary, and, in some cases, tertiary and quaternary structures.<sup>1</sup> Among them,  $\beta$ -peptides are prominent. Their propensity to fold forming sheets, helices and reversed turns has been established.<sup>2</sup> They present the advantage with respect to  $\alpha$ -peptides that the number of residues usually needed to form foldamers is lower than that required in  $\alpha$ -oligomers. In addition, careful design at the residue level can lead to enhanced secondary structural stability among the foldamers relative to conventional peptides. Foldamers with defined folding propensities can be endowed with biological functions, including antibacterial, antifungal and antiviral activities that arise from interaction of the foldamer with a biomolecular partner.<sup>1</sup>

The use of carbocycles<sup>3</sup> and heterocycles<sup>4</sup> incorporated into  $\beta^{2,3}$ -positions of the peptide backbone, combined with the control

of chirality in the monomers, has allowed the synthesis of  $\beta$ -peptides with interesting structural features that include the formation of tertiary structures such as nano-sized fibrils and micelles.<sup>5</sup> The obtained results have allowed a better understanding of the combined influence of chirality and conformational constraint on the molecular and supramolecular arrangement of these compounds. The acquired knowledge has been useful in the preparation of several materials such as nucleic acid mimics<sup>6</sup> and nanotubes.<sup>7</sup>

Although structural features of cyclohexane- and cyclopentane-containing  $\beta$ -peptides are well documented,<sup>3,5</sup> data on the conformational bias and supramolecular structure of  $\beta$ -peptides including four-membered rings are scarce.<sup>8</sup> Fleet *et al.*<sup>4</sup> suggested well-defined left-handed helical structures stabilized by ten-membered hydrogen-bonded rings as the structural preference for  $\beta$ -hexapeptides incorporating *cis*-substituted oxetane rings.<sup>4</sup>

Several types of cyclobutane-containing  $\beta$ -peptides have been synthesized and studied in our laboratory. The ability of the cyclobutane ring to promote defined secondary structures and to self-assemble to form fibrils and gels has been evidenced. Firstly, we reported on  $\beta$ -peptides consisting of cyclobutane residues derived from (1*R*,2*S*)-2-aminocyclobutane-1-carboxylic acid and  $\beta$ -alanine joined in alternation.<sup>9,10</sup> A 14-helical folding was promoted in chloroform solution in a tetrapeptide of this series.<sup>10</sup> Later, we have described the synthesis of a new class of  $\beta$ -peptide starting from (–)-verbenone as a chiral precursor. In these products, the cyclobutane moiety is not a part of the peptide backbone but a bulky substituent at the  $\beta^3$ -position. These products show some conformational bias in solution and, in the solid state, the non-cyclic  $\beta$ -peptides adopt a hairpin-like molecular folding ruled by intermolecular hydrogen bonds in the crystal packing.<sup>11</sup>

<sup>a</sup>Departament de Química, Universitat Autònoma de Barcelona, 08193, Bellaterra, Spain. E-mail: rosa.ortuno@uab.es; Fax: (34) 935811265

<sup>b</sup>Servei de Ressonància Magnètica Nuclear, Universitat Autònoma de Barcelona, 08193, Bellaterra, Spain

<sup>c</sup>Institut de Recerca Biomèdica de Barcelona, Parc Científic de Barcelona, Josep Samitier 1-5, 08028, Barcelona, Spain

<sup>d</sup>Departament de Química Física, Universitat de Barcelona, Martí i Franques 1, 08028, Barcelona, Spain

<sup>e</sup>Departament de Química Orgànica, Universitat de Barcelona, 08028, Barcelona, Spain

† Electronic supplementary information (ESI) available: Details on theoretical calculations, NMR experiments, assigned NMR spectra for **7a**, **8b**, **9a**, **10a**, **12** and **13**, CD spectrum of **8b**, and image of the gel formed by **8b**. See DOI: 10.1039/b918755c

We also prepared and studied a third family of cyclobutane  $\beta$ -peptides derived from different stereoisomers of 2-aminocyclobutane-1-carboxylic acid, **1**, shown in Chart 1. Thus, we reported on the formation of six-membered hydrogen-bonded rings in diastereomeric bis(cyclobutane)  $\beta$ -dipeptides **2** and **3**, in CDCl<sub>3</sub> solution. These intramolecular and intra-residue hydrogen-bonds give rise to *cis*-fused [4.2.0]octane structural units that confer high rigidity on these molecules.<sup>12</sup> We have recently described that this preferred conformation in solution is also

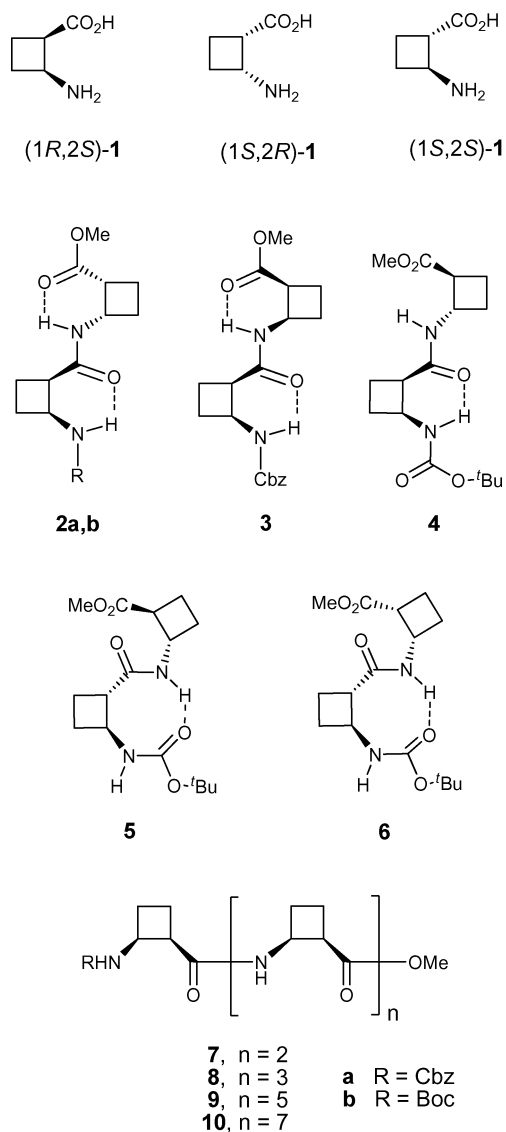
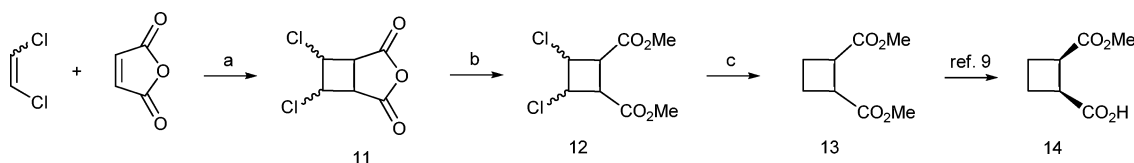


**Chart 1** Structure of some cyclobutane  $\beta$ -amino acids and related  $\beta$ -peptides.



**Scheme 1** Reagents and conditions: (a)  $h\nu$  (quartz), CH<sub>3</sub>CN, -35 °C, 4 h (quantitative); (b) MeOH, H<sub>2</sub>SO<sub>4</sub>, 50 °C, 5 h (88%); (c) H<sub>2</sub> (6 atm), 5% Pd/C, Et<sub>3</sub>N, EtOH, rt (83%).

manifested in  $\beta$ -dipeptide **4**, constituted by residues derived from amino acids (1*R*,2*S*)-**1**, *cis*, and (1*S*,2*S*)-**1**, *trans*, respectively. In contrast, the formation of eight-membered hydrogen-bonded rings prevails in diastereoisomeric dipeptides **5** and **6**.<sup>13</sup>

In a preliminary communication<sup>14</sup> we reported that tetramer **8a** (R = Cbz) showed the same conformational bias in solution as dipeptides **2**, **3** and **4**. Moreover, this compound manifested its tendency to the aggregation forming nano-sized fibres.

On the other hand, cyclobutane-containing  $\beta$ -peptides have become very promising, since recent investigations have revealed their biological activity as a new class of carboxypeptidase inhibitors. Preliminary docking studies show that the conformational constraint imposed by the cyclobutane ring and its small size contribute to suitable interaction with the enzyme.<sup>15</sup>

To gain insight on the structural features of these compounds, in this paper, we present our results on the molecular and supramolecular structures of all-*cis* cyclobutane  $\beta$ -peptides derived from (1*R*,2*S*)-**1**. For this purpose, we have synthesized and studied tetramer **8b** (R = Boc) to ascertain the influence of the protecting group on the conformational bias and self-assembling. Hexamer **9a** and octamer **10a** have been synthesized and investigated to verify if higher oligomers follow the same trends as the smaller ones. Related to these syntheses, we provide herein an improved methodology to prepare the *meso* compound **13** (Scheme 1) in a much cheaper and efficient way. Diester **13** is the starting material to prepare  $\beta$ -amino acids and related peptides<sup>9–10,12–14,16</sup> through an asymmetric and chemoenzymatic hydrolysis to afford half-ester **14**.<sup>9</sup> The conformational analysis of the new  $\beta$ -peptides has been carried out by the combined use of NMR and CD techniques, and computational methods. Tendency to self-assemble has also been explored for dimers **2a,b** as well as for trimer, **7a**, tetramer **8b**, hexamer **9a** and octamer **10a**. A model based on theoretical calculations jointly with transmission electron microscopy (TEM), atomic force microscopy (AFM) and scanning polarization force microscopy (SPFM), is provided to understand the way in which supramolecular aggregation takes place in this family of  $\beta$ -peptides constituted by cyclobutane residues with *cis* configuration.

## Results and discussion

### 1. Synthesis of the oligomers

Half-ester **14** (Scheme 1) is the common chiral precursor to synthesize cyclobutane  $\beta$ -amino acids and  $\beta$ -peptides according to protocols developed in our laboratory.<sup>9,10,12–14</sup>

The simple way to prepare **14** in two steps, which involves esterification and subsequent chemoenzymatic hydrolysis,<sup>9</sup> is from commercially available cyclobutane-1,2-dicarboxylic diacid. Nevertheless, the price of this compound is very high and for this

reason we have established a new synthetic sequence to prepare diester **13**, as shown in Scheme 1.

This synthetic route is inspired by the method reported by Huet *et al.* to prepare dimethyl cyclobut-3-ene-1,2-dicarboxylate.<sup>17</sup> Photochemical [2 + 2] cycloaddition of 1.5 equivalents of 1,2-dichloroethylene (mixture of isomers) to maleic anhydride in a 0.08 M solution of acetonitrile, at  $-35\text{ }^{\circ}\text{C}$ , quantitatively provided the photoadduct **11** as a diastereoisomeric mixture. The lack of stereoselectivity is not relevant since chlorine atoms are removed in a later synthetic step. A similar mixture was obtained by Huet *et al.* who described this cycloaddition to occur in a Pyrex reactor in the presence of benzophenone as a photosensitizer and by using ethyl acetate as a solvent.<sup>17</sup> In our laboratory, better results were achieved in the absence of a photosensitizer, working with a quartz reactor and by using acetonitrile as a solvent. In the next step, Fisher esterification of **11** in refluxing methanol produced dichloro diester **12** (mixture of diastereomers, 88% yield), which was submitted to hydrogenation in the presence of 5% Pd on charcoal under 6 atmospheres pressure resulting in *meso*-diester **13** as the only defined product, in 83% yield after purification. Another synthesis of **13** is described in the literature<sup>18</sup> *via* the photocycloaddition of ethylene to maleic anhydride by using a Pyrex filter.<sup>19</sup> Nevertheless, we found that 4–6 g batches of diester **13** are easily prepared in three steps and in 60% overall yield as shown in Scheme 1. This allows us to avoid the manipulation of a large excess of ethylene as a gas reagent and with a 20-times cheaper cost than the product from commercial sources.

Desymmetrization of **13** was achieved by using pig liver esterase to afford stereoselectively chiral half-ester **14**.<sup>9</sup> Conversion of this compound into fully protected derivatives of monomer (1*R*,2*S*)-**1** was achieved by transformation of the carboxyl group into an intermediate acyl azide and subsequent Curtius rearrangement in the presence of benzyl or *tert*-butyl alcohol (series **a** and **b**, respectively).<sup>10</sup>

Regarding the synthesis of the polycyclobutane  $\beta$ -peptides, dimer **2b**<sup>12</sup> was used in the convergent synthesis of tetramer **8b** through selective deprotection of the amine and the carboxylic acid, respectively (Scheme 2). Peptide coupling of the resultant intermediates in the presence of pentafluorophenyl diphenyl phosphinate (FDPP) produced **8b** in 60% yield.

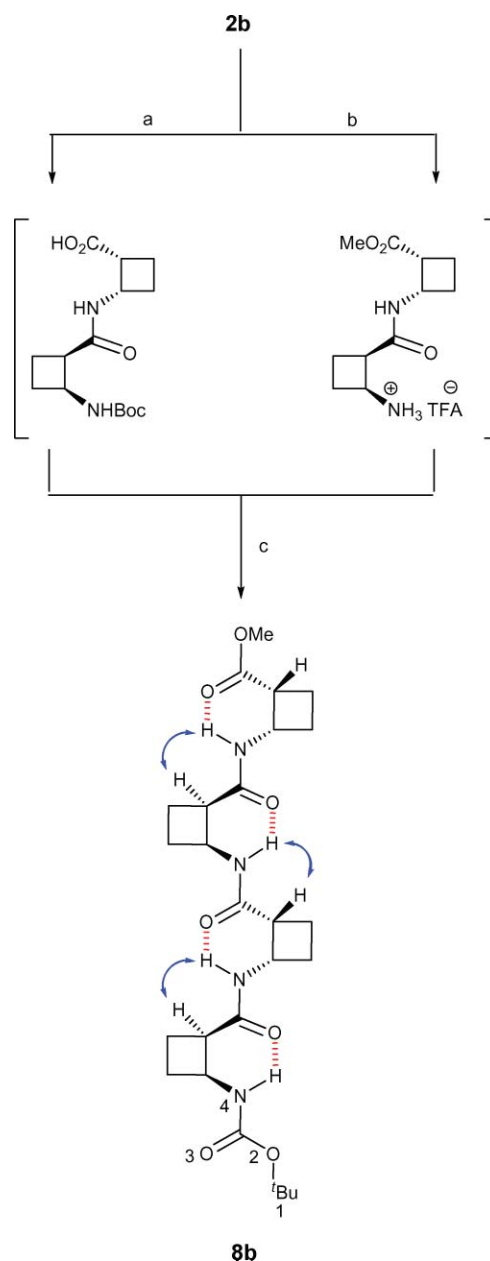
Additionally, hydrogenolysis of benzyl carbamate in dimer **2a** gave amine **15**,<sup>14</sup> which reacted with carboxylic acid **16**<sup>9,12</sup> (Scheme 3) under coupling conditions by using EDAC as a dehydrating agent and hydroxybenzotriazole as a catalyst, in DMF. In this way, the new  $\beta$ -tripeptide **7a** was obtained in 40% yield. In an alternative manner, this product was synthesized *via* the Curtius rearrangement of acyl azide **18** in boiling toluene to afford an isocyanate, which reacted *in situ* with carboxylic acid **17** to provide trimer **7a** in 52% yield with concomitant loss of carbon dioxide.<sup>12</sup> Subsequent selective deprotection of the amine and the carboxylic acid followed by coupling of the resulting compounds resulted in hexamer **9a** in 45% yield (Scheme 3).

Similarly, octamer **10a** was prepared by coupling of two tetrameric units, an amine and a carboxylic acid, derived from **8a**.

## 2. Conformational analysis in solution

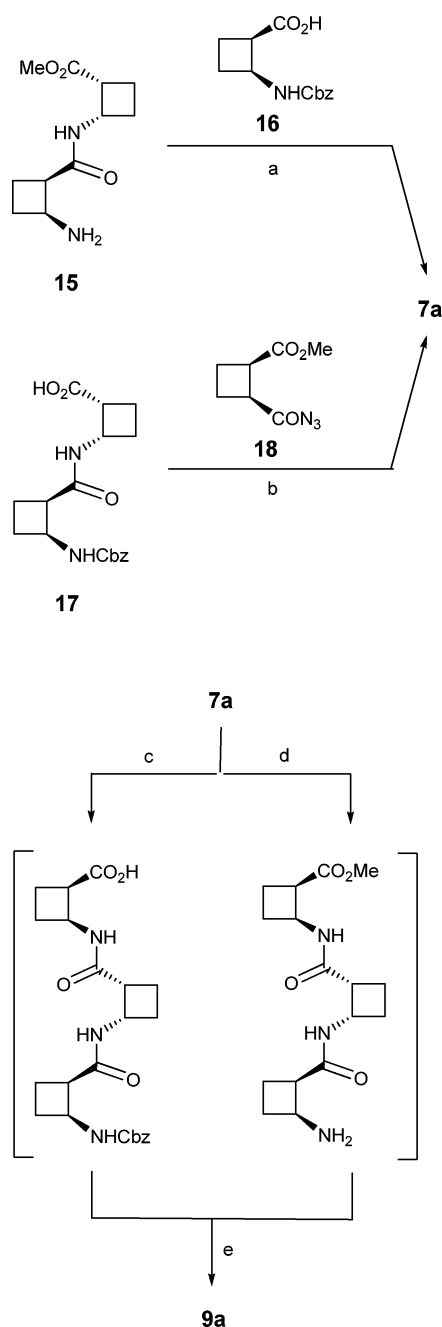
### 2.1 Experimental studies by using NMR and CD techniques.

NMR experiments were carried out on  $\text{CDCl}_3$  solutions. This



**Scheme 2** Reagents and conditions: (a) 0.25 M NaOH (94%); (b) TFA,  $\text{Et}_3\text{SiH}$  (95%); (c) FDPP, DIPEA, DMF (60%).

solvent is suitable for conformational analysis of the target oligomers and has been successfully used in structural studies of related cyclobutane  $\beta$ -peptides.<sup>10–14</sup> In  $\text{CDCl}_3$ , standard 1D and 2D high resolution correlation NMR spectra of tetramer **8b** and hexamer **9a** allowed us to assign all protons and carbon atoms (see the ESI†). Specifically, 2D  $^1\text{H}$ - $^1\text{H}$  NOESY experiments permitted to establish intra- and inter-residue NOE connectivities. Some of these NOE contacts and HH coupling constants led us to secure a *trans* stereochemistry for all amide bonds in the major conformer for each peptide. In the NH region of the  $^1\text{H}$  NMR spectrum, additional signals were observed, which could be attributed to minor conformers arising from rotation around the  $\text{O}=\text{C}-\text{NH}(n+1)$  bond in the carbamate. Particularly significant are the strong inter-residue NOE contacts involving



**Scheme 3** Reagents and conditions: (a) EDAC, HOBT, Et<sub>3</sub>N, DMF (40%); (b) Et<sub>3</sub>N, toluene, reflux (52%); (c) 0.25 M NaOH (70%); (d) H<sub>2</sub> (6 atm), 20% Pd(OH)<sub>2</sub>/C (quantitative); (e) EDAC, HOBT, Et<sub>3</sub>N, DMF (45%).

H $\alpha(i)$  and NH( $i+1$ ) protons since they confirmed a well-defined strand-type conformation both for tetramer **8b** (Scheme 2) and hexamer **9a** (Fig. 1).

This predominant conformation is similar to that found for tetramer **8a** and dimers **2a,b** and is in excellent agreement with the results of theoretical calculations (*vide infra*).

When tetramer **8b** is protected with a Boc group instead of Cbz as in **8a**, it is observed that the NH4 signal becomes broad and loses its doublet structure. This indicates a slight loss of rigidity in the extreme of the strand-type conformation, suggesting that the hydrogen bond is not formed in this segment. Nevertheless,

when the sample is cooled down to 288 K the doublet structure is recovered and the strand-type conformation becomes completely fixed (see Fig. S8 in the ESI<sup>†</sup>). Thus, the emerging conclusion is that the Boc protecting group permits rotation around the O=C $n$ -NH( $n+1$ ) in the carbamate, while Cbz does not.

Comparison of the CD spectra in MeOH for the oligomers of this series (R = Cbz) account for the same preferential conformation in these  $\beta$ -peptides. Fig. 2 shows the superposition of CD spectra of 0.5 mM solutions of dimer **2a**, tetramer **8a**, hexamer **9a** and octamer **10a**. The wavelength is shifted from 210 (**2a**) to 225 nm (**10a**). The intensity is enhanced from **2a** to **9a**, according to the increasing number of chromophores, although the band for the octamer **10a** is similar in intensity to that of tetramer **8a**. Additionally, the normalized (per residue) CD spectra of these oligomers show bands with very close intensities for **2a**, **8a**, and **9a**, whereas the band for **10a** is weaker (Fig. S28 in the ESI<sup>†</sup>). This would be in accordance with a greater flexibility in **10a** than in shorter oligomers. On the other hand, CD spectrum of a 0.5 mM solution of tetrapeptide **8b** (R = Boc) compares well with that of **8a** (see Fig. S26 in the ESI<sup>†</sup>).

## 2.2 Computational studies: simulated annealing (SA) and molecular dynamics (MD).

To begin with, conformational search calculations for **8a**, **9a** and **10a** were done based on SA methodology followed by geometry optimization. The three  $\beta$ -peptides were studied by means of principal components analysis (PCA)<sup>20</sup> to obtain their most representative conformations. The study concluded that the flexibility in the series and, therefore, the total number of conformations increases from **8a** to **10a** as a consequence of the growing number of residues in the  $\beta$ -peptides. Three structures have been selected for each  $\beta$ -peptide **8a**, **9a** and **10a** on the basis of the analysis of the PCA plots. As an example, the three selected conformations, I–III, for the hexapeptide **9a** are shown in Fig. 3.

Subsequently, the dynamic behaviour of the three selected structures obtained by SA for each oligomer was explored by means of MD calculations<sup>21</sup> employing a cubic-box chloroform-solvent model (see Fig. S3 and S4 in the ESI<sup>†</sup>). For each peptide, the three MD calculations converge to similar results, showing the formation of a strand-type conformation in solution. For instance, for hexamer **9a**, the average measured distances between the hydrogens involved in NOE contacts oscillate in values around  $2.30 \pm 0.30$  Å (Table 1), which are in total accordance with the NMR results. Moreover, the calculated NH...O=C distances, in the range of  $2.45 \pm 0.24$  Å, are compatible with the formation of six intramolecular hydrogen bonds as shown in Fig. 1. Fig. 4 shows the average conformation obtained from each trajectory for hexamer **9a**.

MD calculations done for the selected structures of tetrapeptide **8a** and octapeptide **10a** show the same preferential conformation in chloroform solution (see ESI). This conclusion is in good accordance with the most stable conformer previously predicted for tetramer **8a** when results of the conformational search were optimized in chloroform solution at the B3LYP/6-31G(d) level of calculation.<sup>14</sup>

This conformational bias contrasts with the helical structures suggested by Fleet *et al.* for  $\beta$ -hexapeptides containing *cis*-substituted oxetanes.<sup>4</sup> The presence of the oxygen ring as well as

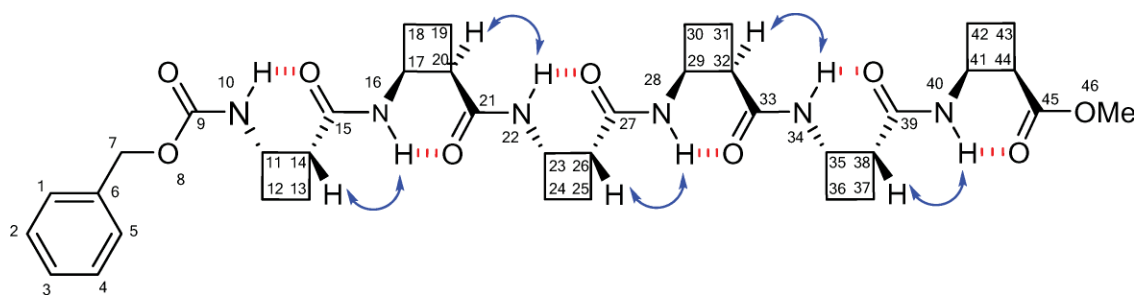


**Fig. 1** Strand-type conformation for hexamer **9a** in  $\text{CDCl}_3$  solution. Arrows show inter-residue  $\text{Ha}(i)$  and  $\text{NH}(i+1)$  NOE contacts.

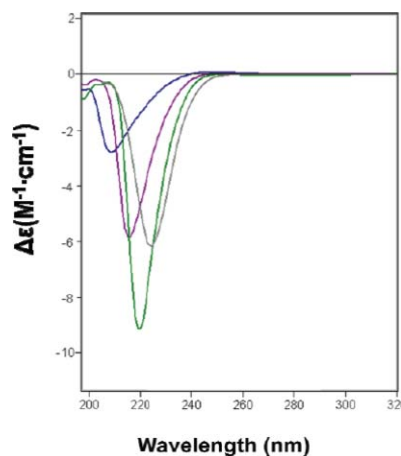


**Fig. 2** CD spectra of 0.5 mM methanol solutions of **2a** (blue), **8a** (violet), **9a** (green), and **10a** (grey).

the additional substituents on the oxetanes could account for the structural differences between cyclobutane and oxetane oligomers.

Strand-type preferential conformation had been previously reported by Fülöp *et al.*<sup>3</sup> for *cis*-2-aminocyclopentanecarboxylic acid oligomers. So, we can conclude that the restriction of the  $\text{NH}-\text{C}^\beta-\text{C}^\alpha-\text{CO}$  torsion in the *gauche* position facilitates extended strand conformations in both cyclobutane and cyclopentane derivatives.

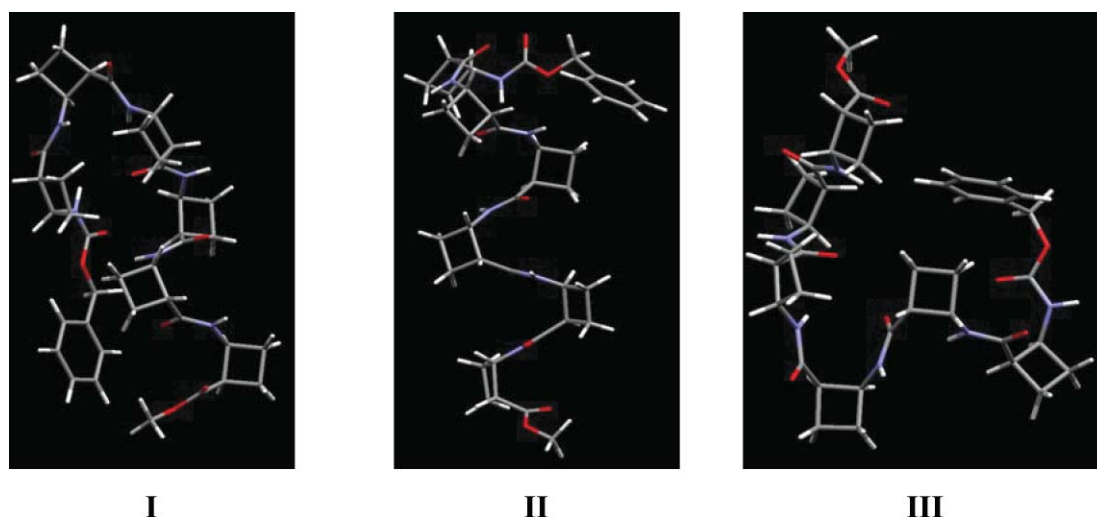
### 3. Aggregation studies

The behaviour of all oligomers of this series was investigated in order to verify their propensity to form aggregates. Although tetramers **8a** and **8b**, hexamer **9a**, and octamer **10a** were obtained as crystals, they were not suitable for structural analysis by X-ray diffraction.

Tetramer **8a** formed an organogel, which was stable for several days, when dissolved in 3:2 ethyl acetate–hexane 1 mM solution by boiling, then air cooling and left to stand. In addition to this, a gel was obtained from 3:1 acetone–hexane 1 mM solution. Unfortunately, it was less stable in this medium and precipitated after standing for 1 d both at room temperature and at 5 °C.<sup>14</sup> Similarly, tetrapeptide **8b** formed a stable gel from 1:3 dichloromethane–pentane 5.8 mM solution at 25 °C (see Fig. S27 in the ESI†).

All  $\beta$ -peptides in this series show strong tendency to self-assemble from methanol solutions giving nanosized fibres whose morphology remained unaltered after one week incubation. Fig. 5 shows selected images of fibres from different oligomers, obtained under the optimal conditions in each case.

In the case of **10a**, TEM images of 0.5 M solutions after 24 h incubation revealed the formation of homogeneous vesicles, which remained unaltered at room temperature for, at least, two weeks. Their diameters measured from 70 to 100 nm on average (Fig. 6a). Aggregates with fibrillar morphology were observed from 1 mM solutions after a one week incubation period (Fig. 6b).

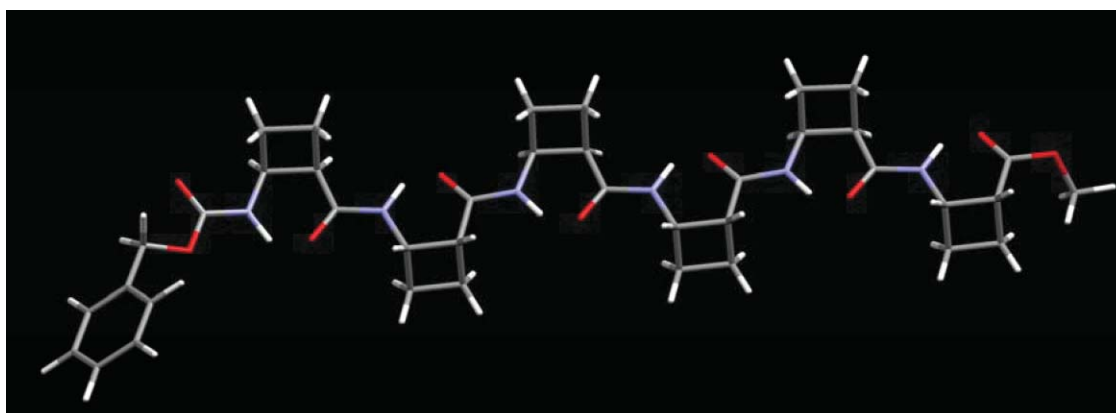
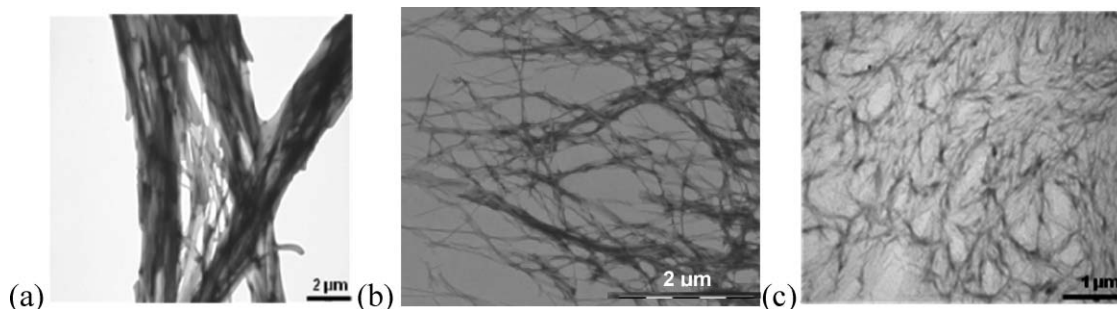


**Fig. 3** Selected conformers for hexamer **9a**.

**Table 1** MD calculated average  $H\alpha(i) \cdots NH(i+1)$  and  $NH(n) \cdots OC(n)$  distances <sup>a</sup> for the three trajectories of hexamer **9a**<sup>b</sup>

Conformer	H14 $\cdots$ NH16	H20 $\cdots$ NH22	H26 $\cdots$ NH28	H32 $\cdots$ NH34	H38 $\cdots$ NH40	
<b>I</b>	2.32	2.32	2.28	2.43	2.28	
<b>II</b>	2.36	2.28	2.31	2.34	2.38	
<b>III</b>	2.23	2.38	2.32	2.29	2.35	
Conformer	NH10 $\cdots$ OC15	NH16 $\cdots$ OC21	NH22 $\cdots$ OC27	NH28 $\cdots$ OC33	NH34 $\cdots$ OC39	NH40 $\cdots$ OC45
<b>I</b>	2.58	2.67	2.70	2.77	2.15	2.05
<b>II</b>	2.44	2.60	2.69	2.64	2.46	1.92
<b>III</b>	2.37	2.58	2.57	2.42	2.44	2.14

<sup>a</sup> In angstroms. <sup>b</sup> See Fig. 1 for atom numeration.

**Fig. 4** Image showing the average strand-type conformation obtained from each MD calculation for the three trajectories of hexamer **9a**.**Fig. 5** TEM images of the nanosized fibres formed by (a) **2a** from a 5 mM, (b) **8b** from a 1 mM, (c) **9a** from a 0.5 mM solution in MeOH (1 d incubation) placed onto a carbon film-coated copper grid and stained with 2% uranyl acetate.

Accordingly, higher concentration account for the evolution from vesicles to fibrils in MeOH solutions of **10a**. A similar behaviour has been observed for other peptides.<sup>22</sup> Self-assembled peptide-based vesicles have been used for biological purposes such as DNA delivery and release in cells.<sup>22</sup>

In addition, AFM of tetrapeptide **8a** onto a mica substrate showed the formation of monolayers, which, after longer periods of time, pile themselves up into a multilayer structure. Fig. 7a shows a topographic image of **8a** molecules. The heights measured range from 6.4 to 8.8 ( $\pm 0.2$ ) nm with a periodicity of 2.2 nm, which is in agreement with the size of single molecular tetrapeptide **8a**,<sup>14</sup> as represented in Fig. 8.

The local charge distribution of the nanosized fibres was studied by SPFM. While AFM made it possible to gain information on the structural properties of fibrils, SPFM measurements enabled us to

characterize the local charge distribution of the self-assemblies. It is noteworthy that the surface potential (SP) of the fibrils increased with the size of the self-assemblies, as can be observed in Fig. 7b.

In addition, the calculated dipole moment at the B3LYP/6-31G(d) level of calculation<sup>14</sup> for **8a** is 11.1 D, with the positive pole on the C-terminus. All these results suggest a molecular arrangement as shown in Fig. 8, with the N-terminus oriented towards the surface of the mica substrate.

MD calculations were undertaken to understand the mode of aggregation in the monolayer. These calculations were carried out for two cells containing nine molecules with two different arrangements, parallel and alternate (Fig. 9).

To keep this ordering stable along the whole MD, the eight molecules surrounding the central one are partially

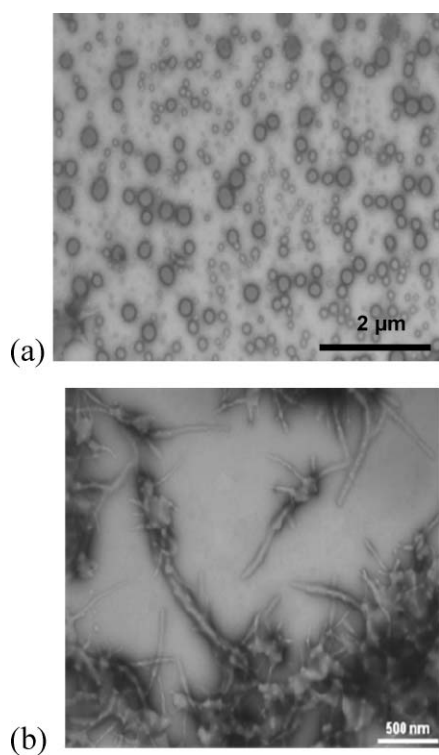


**Fig. 6** Aggregates formed by **10a** from (a) 0.5 mM solution in MeOH after 1 day incubation, and (b) 1mM solution in MeOH after incubation for a week.

retained in their positions by restraints in order to maintain the basic cell. The restrictions were softly included into the system by allowing distance fluctuations of  $\pm 2$  Å from the

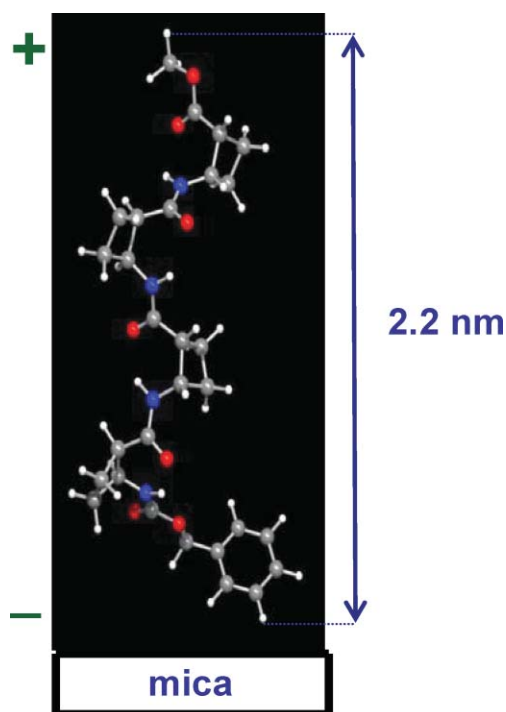


**Fig. 8** Modelled vertical arrangement of the molecules of **8a** in the assemblies, as suggested by AFM and SPFM experiments and the calculated dipole moment.

equilibrium distance. The molecule in the middle is absolutely unrestrained and is therefore able to freely interact with its environment.

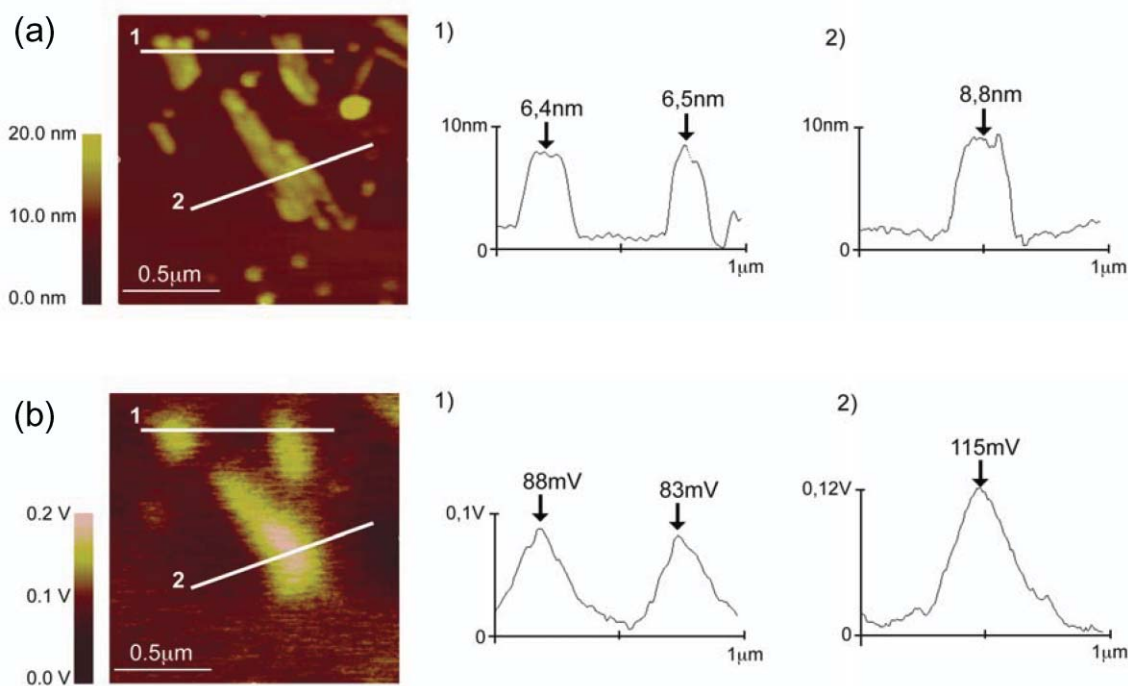


**Fig. 7** (a) Topographic image of tetrapeptide **8a** molecules deposited onto a freshly cleaved mica substrate. The heights measured range from 6.4 ( $\pm 0.2$ ) to 8.8 ( $\pm 0.2$ ) nm. (b) Surface potential (SP) image of the same **8a** molecules deposited onto a freshly cleaved mica substrate. The SP measurements of the nanosized fibres increase with the size of the self-assemblies.

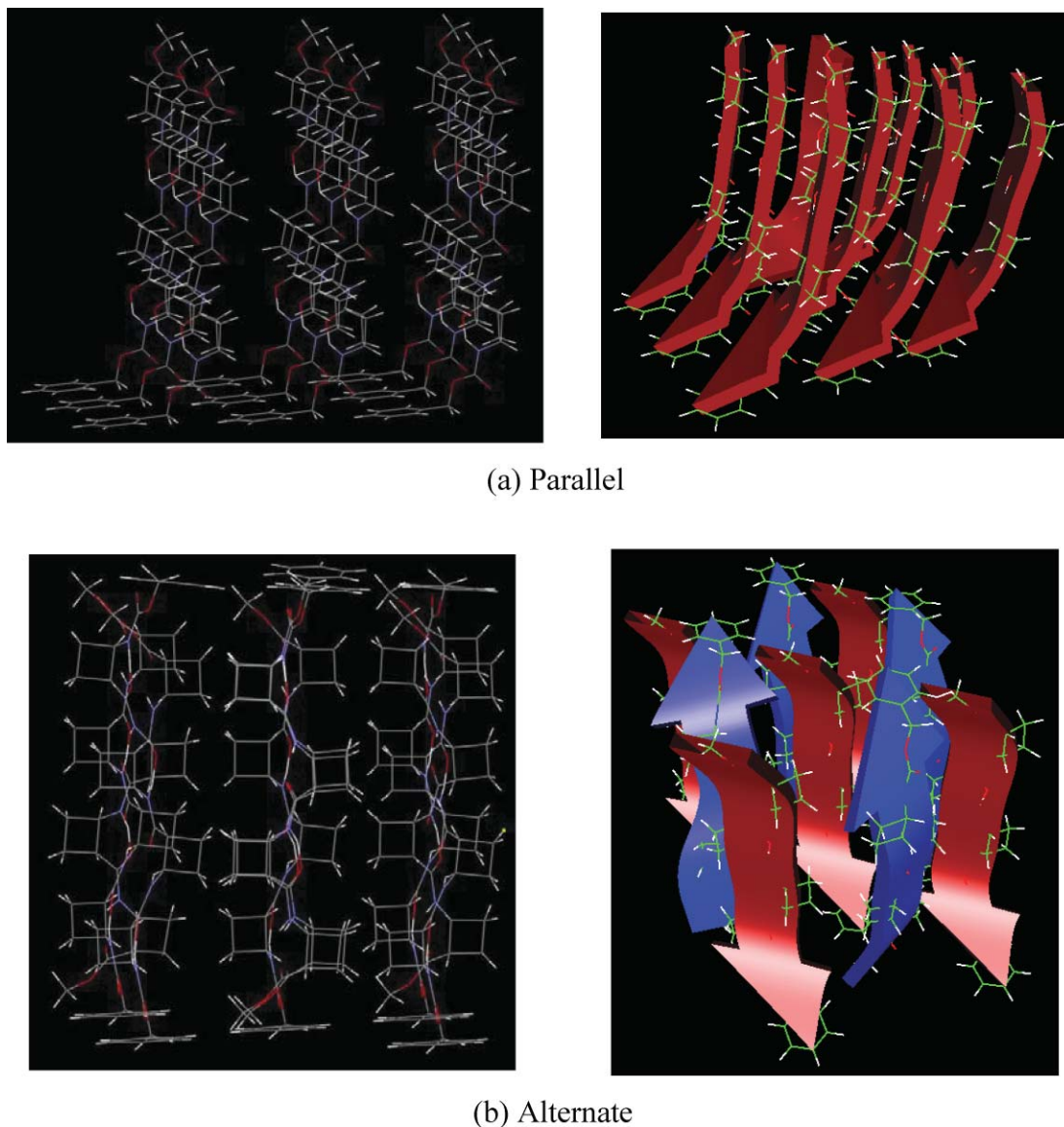


**Fig. 9** Parallel (a) and alternate (b) monolayer arrangements for nine molecules of tetramer **8a**.

The two boxes already built, parallel and alternate, were subjected to MD calculations. The results obtained point out that the system exhibits a preference for the parallel arrangement because of its lower energy (Fig. 10), which is in accordance with SPFM results. Moreover, MD trajectories show that interactions among the nine phenyl groups are quite favoured.

The possible inter and intramolecular hydrogen bonds involving the central peptide molecule were analyzed during the MD calculations (Table 2). The results show that the molecules interact better by hydrogen bonding in the parallel aggregate (44.80%) than in the alternate one (38.78%) (Table 2). This also points out that the parallel monolayer is energetically favoured, which agrees with the results in Fig. 10.

These results show that both inter and intramolecular hydrogen bonds coexist in the aggregates and that the conformation of the peptide reproduces that observed in solution, as shown in Fig. 11.

All these results suggest that both hydrophilic (hydrogen bonding) and hydrophobic interactions account for the supramolecular

arrangements of tetramer **8a**. This model could be applied to the other oligomers in the all-*cis* series.

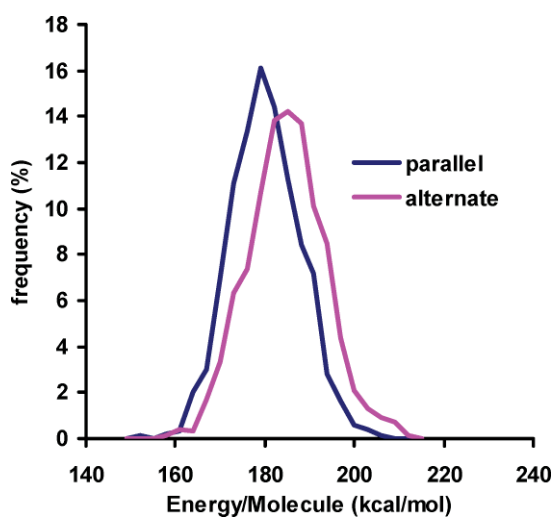
## Conclusions

High-resolution NMR experiments, CD spectra and computational studies reveal that  $\beta$ -peptides constituted by residues derived from (1*R*,2*S*)-2-aminocyclobutane-1-carboxylic acid adopt a strand-type conformation in solution, independently of their size and the terminal amine protecting group. The presence of the small cyclobutane ring imposes this conformational bias, which results from the formation of intra-residue hydrogen-bonded six-membered rings giving rise to *cis*-fused [4.2.0]octane structural units that confer high rigidity on these  $\beta$ -peptides. This result compares well with a similar conformation described in the literature for oligomers consisting of *cis*-2-aminocyclopentanecarboxylic acid residues. In both cases, the NH-C <sup>$\beta$</sup> -C <sup>$\alpha$</sup> -CO torsion restricted in the *gauche* position



**Table 2** Statistical probability for hydrogen bonding in the parallel and the antiparallel arrangements

Box type	Molecular interaction	Number ( <i>N</i> )	Frequency (%)	NH...O=C distance/Å	N-H-O angle (°)
Parallel	Inter	14	20.70	3.32	40.94
	Intra	5	24.10	3.04	51.50
	Total	19	44.80	3.25	43.73
Alternate	Inter	8	28.83	3.30	43.30
	Intra	5	9.95	2.04	51.97
	Total	13	38.78	3.20	46.63

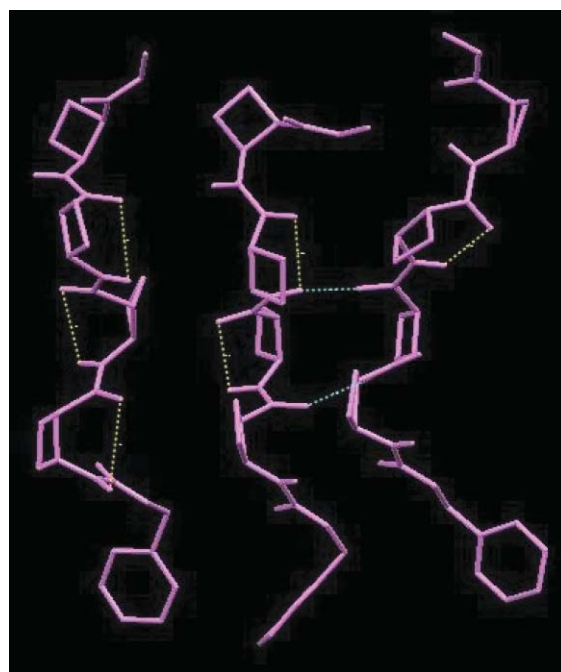
**Fig. 10** Energy histograms for the parallel and alternate monolayer arrangements of tetramer **8a**.

favours such a conformation. Otherwise, the propensity of *cis*-cyclobutane  $\beta$ -oligomers to self-assemble and produce nanosized fibres has been evidenced by TEM, AFM and SPFM. The results given by these techniques and molecular modelling based on theoretical calculations suggest a parallel alignment as the preferential molecular arrangement in the aggregates and a molecular conformation similar to that observed in solution. In the assemblies, both hydrogen bonding and hydrophobic interactions could be responsible for the aggregation. In addition, tetramers are able to produce gels in some organic solvents. The nature of the *N*-protecting group does not exert a strong influence on these features. All these properties confer a great interest on these compounds. Consequently, the synthesis and structural study of new  $\beta$ -peptides including cyclobutane residues with diverse stereochemistry, and also hybrid oligomers combining cyclic and linear units is currently in progress in our laboratory. In light of some promising results,<sup>15</sup> the search for their possible biochemical applications as well as their use in the design of new chiral materials is under active investigation.

## Experimental

### Computational Details

The molecules **8a–10a** were built taking profit of the modular philosophy of AMBER 7,<sup>23</sup> and the parm99<sup>24</sup> Force Field was employed in all cases. Several auxiliary software packages are used to carry out side calculations such as MacroModel 9.0<sup>25</sup>

**Fig. 11** Single MD parallel snapshot showing the arrangement of two neighboring molecules with respect to the unrestrained central one in the aggregates formed by **8a**. Significant intra and intermolecular hydrogen bonds are marked. The three molecules adopt an extended arrangement like the predominant conformation of **8a** in chloroform solution.

(geometrical optimizations) and Gaussian 98<sup>26</sup> (determining Merz–Kollman atomic charges). Simulated Annealing<sup>27</sup> methodology (5000 steps, time-step 1.0 fs, SHAKE<sup>28</sup> protocol and variable thermal coupling<sup>29</sup>) was employed followed by geometrical optimization (Steepest Descent<sup>30</sup> algorithm for the first 10 steps and then Conjugated Gradient<sup>31</sup> algorithm until full convergence). Detailed conditions are included in the SA.in file (for a deep insight consult Fig. S2 and file SA in the ESI†). Molecular dynamics calculations were also done with the AMBER 7 software package according to a schema in 3 steps, explained in Figure S4 (see the ESI†): previous step involving geometrical optimization and then; 300 ps. NVT heating step; 300 ps. NPT equilibration step; and 5000 ps. NPT sampling step (sampling ratio: 1 frame per ps. Time-step: 1.0 fs). The calculations for the parallel and the alternate arrangements were done according to a scheme (see the ESI, Fig. S5†): a first step involving geometrical optimization followed by a 500 ps heating and equilibration step and, finally, a 10000 ps. sampling step (sampling ratio: 1 frame per 10 ps. Time-step 1.0 fs). Calculations were done in vacuum assuming

that any molecule, once the aggregate has formed, only feels in its vicinity other molecules similar to it and not any trace of solvent.

### 6,7-Dichloro-3-oxabicyclo[3.2.0]heptane-2,4-dione **11**<sup>17</sup>

A solution of maleic anhydride (2 g, 20.6 mmol) in acetonitrile (250 mL) was cooled to  $-35\text{ }^{\circ}\text{C}$ . (*Z*)-1,2-dichloroethylene (2.3 mL, 30.9 mmol) was added and the system was irradiated through a quartz filter for 4 h. The solvent was removed *in vacuo* to afford pure compound **11** as a white solid, as a mixture of diastereomeric adducts (3.98 g, quantitative yield). The  $^1\text{H}$  NMR spectrum of the mixture is in good agreement with that previously described for these compounds.<sup>17</sup>  $\delta_{\text{H}}$ (250 MHz;  $\text{CDCl}_3$ ) 4.30–4.34 (complex absorption, 2H) and 5.47–5.51 (complex absorption, 2H) (one adduct). 3.85–3.91 (m, 1H), 4.40–4.49 (m, 1H) and 5.10–5.19 (complex absorption, 2H) (one adduct). 4.07–4.09 (complex absorption, 2H) and 5.39–5.40 (complex absorption, 2H) (one adduct).

### Dimethyl 3,4-dichlorocyclobutane-1,2-dicarboxylate **12**<sup>17</sup>

A solution of cycloadduct mixture **11** (8.5 g, 43.6 mmol) and concentrated  $\text{H}_2\text{SO}_4$  (1.7 mL) in methanol (85 mL) were stirred at  $50\text{ }^{\circ}\text{C}$  for 5 h. Dichloromethane (150 mL) was added to the organic phase and it was successively washed with water ( $2 \times 100\text{ mL}$ ) and brine ( $1 \times 100\text{ mL}$ ). The organic layer was then dried over  $\text{MgSO}_4$ , filtered off and concentrated in order to provide the corresponding crude as yellowish oil (9.2 g, 88% yield).  $\delta_{\text{H}}$ (250 MHz;  $\text{CDCl}_3$ ) 3.20–3.28 (dd,  $J = 9.25\text{ Hz}$ , 1H), 3.69–3.71 (complex absorption, 2H), 3.74 (s, 6H), 3.75 (s, 3H), 3.76 (s, 6H), 3.77 (s, 3H), 3.78–3.81 (complex absorption, 2H), 3.89 (ddd,  $J = 9.2\text{ Hz}$ ,  $J' = 10.1\text{ Hz}$ , 1H), 4.37–4.44 (dd,  $J = 8\text{ Hz}$ ,  $J' = 9.1\text{ Hz}$ , 1H), 4.83–4.96 (complex absorption, 5H).

### Dimethyl cyclobutane-1,2-dicarboxylate **13**<sup>9</sup>

TEA (8.1 mL, 9.7 mmol) was added to a solution of **12** (6.4 g, 26.5 mmol) in ethanol (15 mL). The mixture was hydrogenated over 5% Pd/C (2.6 g) at room temperature and at 6 atm for 58 h. The catalyst was removed by filtration through Celite® and washed successively with methanol and dichloromethane. The filtrate was evaporated *in vacuo*. The residue was the residue poured into EtOAc (100 mL) and the resultant solution was washed twice with saturated aqueous  $\text{NaHCO}_3$  (100 mL). The organic layer was dried over  $\text{MgSO}_4$ , filtered off and solvent removed to provide **13** (3.9 g, 85% yield).  $\delta_{\text{H}}$ (250 MHz;  $\text{CDCl}_3$ ) 2.19 (m, 2H), 2.39 (m, 2H), 3.40 (m, 2H), 3.68 (s, 3H);  $\delta_{\text{C}}$  (62.5 MHz;  $\text{CDCl}_3$ ) 22.2 (2C), 40.7, 51.7 (2C), 173.9 (2C).

### Procedures for the synthesis of peptides. Method A: peptide coupling with EDAC

As an example, the synthesis of hexapeptide **9a** is described. Tripeptide **7a** (200 mg, 0.43 mmol) was dissolved in 1 : 2 THF–water (16 mL) and 0.25 M NaOH (4.5 mL) was added. The mixture was stirred at  $0\text{ }^{\circ}\text{C}$  for 4.5 h, then washed with  $\text{CH}_2\text{Cl}_2$  ( $3 \times 15\text{ mL}$ ) before being acidified to pH 2 with 2M HCl. The aqueous layer was extracted with EtOAc ( $4 \times 40\text{ mL}$ ) and the organic layer was

dried over  $\text{MgSO}_4$ , filtered and evaporated under high vacuum, obtaining the corresponding carboxylic acid (133.5 mg, 70%). This compound was used directly in next step without further purification.

On the other hand, tripeptide **7a** (200 mg, 0.43 mmol) was dissolved in EtOH (30 mL) and 20%  $\text{Pd}(\text{OH})_2/\text{C}$  was added (70 mg). The mixture was stirring under hydrogen ( $P = 6\text{ atm}$ ), at room temperature for 12 h. After that, the catalyst was removed by filtering through Celite® and washed with MeOH. Then the resulting mixture was concentrated under reduced pressure to obtain quantitatively the free amine as a yellowish oil, which was used in next step without further purification.

After that, the free carboxylic acid (120 mg, 0.27 mmol) and the free amine (100 mg, 0.3 mmol) were dissolved in anhydrous DMF (25 mL). Then, TEA (0.23 mL), EDAC (175 mg, 0.91 mmols) and HOBt (60 mg, 0.44 mmols) were successively added. The mixture was stirred for 20 d under a nitrogen atmosphere. After EtOAc was added (25 mL) and organic layer was washed with aqueous saturated solution of  $\text{NaHCO}_3$  ( $3 \times 20\text{ mL}$ ), dried over  $\text{MgSO}_4$  and concentrated under reduced pressure. The obtained crude product was purified by flash column chromatography through Baker silica gel using EtOAc as eluent, to afford the hexapeptide **9a** (91 mg, 45%) as a white solid.

**Hexapeptide 9a.** Crystals, mp  $173\text{--}175\text{ }^{\circ}\text{C}$  (EtOAc–pentane);  $[\alpha]_{\text{D}}^{25} -153.0$  ( $c\ 0.57$ , MeOH);  $\nu_{\text{max}}(\text{ATR})/\text{cm}^{-1}$  3297, 2944, 1718, 1643;  $\delta_{\text{H}}$ (500 MHz;  $\text{CDCl}_3$ ) 1.90–2.34 (complex absorption, 24H), 3.14 (complex absorption, 5H), 3.41 (m, 1H), 3.73 (s, 3H), 4.49 (m, 1H), 4.66–4.77 (complex absorption, 5H), 5.07 (dd,  $J = 10\text{ Hz}$ ,  $J' = 25\text{ Hz}$ , 2H), 5.99 (d,  $J = 10\text{ Hz}$ , 1H), 6.52 (d,  $J = 10\text{ Hz}$ , 1H), 6.73–6.83 (complex absorption, 4H), 7.35 (complex absorption, 5H);  $\delta_{\text{C}}$ (125 MHz;  $\text{CDCl}_3$ ) 19.0–19.4, 29.1–30.0, 43.9, 44.1–44.3, 44.4, 45.5, 46.0, 46.2, 51.8, 66.5, 127.9, 128.5, 136.6, 155.6, 172.2–172.6;  $m/z$  (ESI): Found, 771.3688  $[\text{M} + \text{Na}]^+$ . Calcd. for  $\text{C}_{39}\text{H}_{52}\text{N}_6\text{O}_9\text{Na}$ : 771.3688.

**Octapeptide 10a.** Following a similar protocol than that described above for hexapeptide **9a**, octapeptide **10a** was prepared from tetramer **8a**. 70 mg, 35% yield. Crystals, mp  $188\text{--}190\text{ }^{\circ}\text{C}$  (EtOAc–pentane);  $[\alpha]_{\text{D}}^{25} -110.0$  ( $c\ 0.74$ ,  $\text{CH}_2\text{Cl}_2$ );  $\nu_{\text{max}}(\text{ATR})/\text{cm}^{-1}$  3299, 2949, 1715, 1648;  $\delta_{\text{H}}$ (500 MHz;  $\text{CDCl}_3$ ) 1.80–2.42 (complex absorption, 32H), 3.11–3.45 (complex absorption, 8H), 3.70 (s, 3H), 4.47 (m, 1H), 4.64–4.79 (complex absorption, 7H), 5.10 (m, 2H), 5.98 (m, 1H), 6.53 (d,  $J = 7\text{ Hz}$ , 1H), 6.70–6.92 (complex absorption, 6H), 7.34 (complex absorption, 5H);  $\delta_{\text{C}}$ (125 MHz;  $\text{CDCl}_3$ ) 18.9–19.6, 28.8–29.2, 43.9–46.3, 51.7, 66.5, 127.9, 128.4, 136.6, 155.5, 172.0–173.0, 174.6;  $m/z$  (MALDI-TOF): Found, 965.561  $[\text{M} + \text{Na}]^+$ . Calcd. for  $\text{C}_{49}\text{H}_{66}\text{N}_8\text{O}_{11}\text{Na}$ : 965.475.

### Method B: peptide coupling with FDPP

The synthesis of tetrapeptide **8b** is described. On one hand, dipeptide **2b** (100 mg, 0.31 mmol) was solved in 1 : 10 THF–water (22 mL) and 0.25 M NaOH (3 mL) was added. The mixture was stirred at  $0\text{ }^{\circ}\text{C}$  for 2 h. The mixture was washed with  $\text{CH}_2\text{Cl}_2$  ( $2 \times 15\text{ mL}$ ) before being acidified to pH 2 with 2M HCl. The aqueous layer was extracted with EtOAc ( $4 \times 40\text{ mL}$ ) and the organic layer was dried over  $\text{MgSO}_4$ , filtered and evaporated under high vacuum obtaining the corresponding carboxylic acid (90 mg,

94%). This compound was used directly in next step without further purification.

On the other hand, dipeptide **2b** (140 mg, 0.43 mmols) was solved in dry  $\text{CH}_2\text{Cl}_2$  (10 mL) and  $\text{Et}_3\text{SiH}$  (0.17 mL, 1.10 mmol) and TFA (0.43 mL, 5.60 mmol) were added. The mixture was stirred at room temperature for 2 h. The reaction mixture was concentrated under reduced pressure obtaining the free amine as a yellowish oil (90 mg, 95%), which was used in next step without further purification.

After that, a solution containing the free carboxylic acid (0.09 g, 0.29 mmol), the free amine (0.09 g, 0.39 mmol), DIPEA (0.1 mL, 0.48 mmol), and FDPP (0.08 g, 0.19 mmol) in anhydrous DMF (10 mL) was stirred at room temperature overnight. Then, ethyl acetate (40 mL) was added and the combined organic layers were washed with saturated aqueous  $\text{NaHCO}_3$  ( $3 \times 30$  mL). The organic layer was dried over  $\text{MgSO}_4$  and solvents were removed under reduced pressure. The residue was purified by column chromatography using dichloromethane–methanol (29 : 1) as eluent to afford **8b** (90 mg, 60%) as a white solid.

**Tetrapeptide 8b.** Crystals, mp 225–227 °C;  $[\alpha]_{\text{D}}^{25}$  –263.9 (*c* 0.95, MeOH);  $\nu_{\text{max}}$ (ATR)/ $\text{cm}^{-1}$  3349, 3315, 2944, 1727, 1683, 1648, 1515;  $\delta_{\text{H}}$ (600 MHz;  $\text{CDCl}_3$ ) 1.41 (s, 9H), 1.84–2.07 (complex absorption, 8H), 2.15–2.25 (complex absorption, 4H), 2.27–2.34 (complex absorption, 4H), 3.12 (m, 1H), 3.16 (m, 2H), 3.40 (m, 1H), 3.70 (s, 3H), 4.38 (m, 1H), 4.65–4.77 (complex absorption, 3H), 5.59 (d,  $J = 9.4$  Hz, 1H), 6.63 (d,  $J = 8.9$  Hz, 1H), 6.71 (d,  $J = 8.7$  Hz, 1H), 6.75 (d,  $J = 8.7$  Hz, 1H);  $\delta_{\text{C}}$ (150 MHz;  $\text{CDCl}_3$ ) 18.6, 19.2 (3C), 28.4 (3C), 29.1, 29.2, 29.3, 29.7, 44.0, 44.5 (3C), 45.7 (2C), 46.1, 46.3, 51.8, 79.2, 155.1, 172.3, 172.6, 172.7, 174.6; *m/z* (ESI): Found, 543.2793  $[\text{M} + \text{Na}]^+$ . Calcd. for  $\text{C}_{26}\text{H}_{40}\text{N}_4\text{O}_7\text{Na}$ : 543.2789. Anal. Found: C, 59.62; H, 7.76; N, 10.36. Calcd. for  $\text{C}_{26}\text{H}_{40}\text{N}_4\text{O}_7$ : C, 59.98; H, 7.74; N, 10.76.

#### Method C: reaction between a carboxylic acid and an azide<sup>12</sup>

The synthesis of tripeptide **7a** is described. To a solution of acid **17** (300 mg, 0.86 mmol) in dried toluene (10 mL), were added TEA (0.15 mL) and azide **18** (140 mg, 0.76 mmols) dissolved in 15 mL of dried toluene. The reaction mixture was stirred for 6 h at 100 °C. After that, the reaction was quenched with EtOAc and the organic layer was washed with an aqueous saturated solution of  $\text{NaHCO}_3$  ( $3 \times 15$  mL). The combined organic layers were dried over  $\text{MgSO}_4$ , filtered and evaporated. The product was purified by flash column chromatography through Baker silica gel (1 : 1 hexane–EtOAc as eluent) to afford the tripeptide **7a** (180 mg, 52%) as a white solid.

**Tripeptide 7a.** Crystals, mp 190–192 °C (EtOAc–pentane);  $[\alpha]_{\text{D}}^{25}$  –145.7 (*c* 1.64,  $\text{CH}_2\text{Cl}_2$ );  $\nu_{\text{max}}$ (ATR)/ $\text{cm}^{-1}$  3302, 2948, 1700, 1651, 1541;  $\delta_{\text{H}}$ (500 MHz;  $\text{CDCl}_3$ ) 1.96 (m, 6H), 2.12–2.38 (m, 6H), 3.15 (m, 2H), 3.39 (m, 1H), 3.69 (s, 3H), 4.48 (m, 1H), 4.63–4.79 (m, 2H), 5.08 (m, 2H), 5.91 (d,  $J = 7.2$  Hz, 1H), 6.52 (d,  $J = 8.7$  Hz, 1H), 6.65 (d,  $J = 7.2$  Hz, 1H), 7.34 (m, 5H);  $\delta_{\text{C}}$ (125 MHz;  $\text{CDCl}_3$ ) 19.8, 20.1, 20.2, 30.1, 30.2, 30.8, 44.8, 45.3, 45.4, 46.6, 47.0, 47.2, 52.7, 66.5, 128.9, 129.4 (2C), 137.5, 156.3, 173.2, 172.3 175.6. Anal. Found: C, 63.13; H, 6.75; N, 9.19. Calcd. for  $\text{C}_{24}\text{H}_{31}\text{N}_3\text{O}_6$ : C, 63.00; H, 6.83; N, 9.18.

#### Acknowledgements

Authors thank financial support from Spanish Ministerio de Ciencia e Innovación (grants CTQ2007-61704/BQU, CTQ2006-08256) and Generalitat de Catalunya (grants 2009SGR-733 and 109, and XRQTC). They are also grateful to European Union for COST Action CM0803. Time allocated in the Servei de Ressonància Magnètica Nuclear and Servei de Microscòpia Electrònica (UAB), and in CESCA (Centre de Supercomputació de Catalunya) is gratefully acknowledged.

#### Notes and references

- 1 For a definition of secondary and tertiary structures in peptides, see: S. H. Gellman, *Acc. Chem. Res.*, 1998, **31**, 173. For recent reports on helix bundle quaternary structures of  $\beta$ - and  $\alpha/\beta$  peptides, respectively, see: D. S. Daniels, E. J. Petersson, J. X. Qiu and A. Schepartz, *J. Am. Chem. Soc.*, 2007, **129**, 1532; W. S. Horne, J. L. Price, J. L. Keck and S. H. Gellman, *J. Am. Chem. Soc.*, 2007, **129**, 4178; S. H. Gellman, Abstracts of Papers, 237th ACS National Meeting, Salt Lake City, UT, United States, 2009.
- 2 See, for example: M. A. Gellman, and S. H. Gellman, in *Enantioselective Synthesis of  $\beta$ -Amino Acids*, Second Edition, ed. E. Juaristi and V. A. Soloshonok, John Wiley and Sons, New Jersey, 2005, pp. 527–585; D. Seebach, D. F. Hook and A. Glattli, *Biopolymers*, 2006, **84**, 23; P. Le Grel and G. Guichard, in *Foldamers: Structure, Properties and Applications*, ed. S. Hecht and I. Huc, Wiley-VCH, Weinheim, 2007, pp. 35–74; D. Seebach and J. Gardiner, *Acc. Chem. Res.*, 2008, **41**, 1366; W. S. Horne and S. H. Gellman, *Acc. Chem. Res.*, 2008, **41**, 1399; I. M. Mándity, E. Wèber, T. Martinek, G. Olajos, G. K. Tóth, E. Vass and F. Fülöp, *Angew. Chem., Int. Ed.*, 2009, **48**, 2171.
- 3 For some representative references, see: D. H. Appella, L. A. Christianson, I. L. Karle, D. R. Powell and S. H. Gellman, *J. Am. Chem. Soc.*, 1996, **118**, 13071; D. H. Appella, L. A. Christianson, I. L. Karle, D. R. Powell and S. H. Gellman, *J. Am. Chem. Soc.*, 1999, **121**, 6206; D. H. Appella, L. A. Christianson, D. A. Klein, M. R. Richards, D. R. Powell and S. H. Gellman, *J. Am. Chem. Soc.*, 1999, **121**, 7574; K. Möhle, R. Günther, M. Thormann, N. Sewald and H.-J. Hofmann, *Biopolymers*, 1999, **50**, 167; J. J. Barchi, Jr., X. Huang, D. H. Appella, L. A. Christianson, S. L. Durrell and S. H. Gellman, *J. Am. Chem. Soc.*, 2000, **122**, 2711; T. A. Martinek, G. Tóth, E. Vass, M. Hollósi and F. Fülöp, *Angew. Chem., Int. Ed.*, 2002, **41**, 1718; R. J. Doerksen, B. Chen, J. Yuan, J. D. Winkler and M. L. Klein, *Chem. Commun.*, 2003, 2534; M. A. Schmitt, S. H. Choi, I. A. Guzei and S. H. Gellman, *J. Am. Chem. Soc.*, 2006, **128**, 4538; F. Fülöp, T. A. Martinek and G. K. Tóth, *Chem. Soc. Rev.*, 2006, **35**, 323.
- 4 See, for instance: T. D. W. Claridge, J. M. Goodman, A. Moreno, D. Angus, S. F. Barker, C. Taillefumier, M. P. Watterson and G. W. Fleet, *Tetrahedron Lett.*, 2001, **42**, 4251.
- 5 A. Hetényi, I. M. Mándity, T. A. Martinek, G. K. Tóth and F. Fülöp, *J. Am. Chem. Soc.*, 2005, **127**, 547; T. A. Martinek, I. M. Mándity, L. Fülöp, G. K. Tóth, E. Vass, M. Hollósi, E. Forró and F. Fülöp, *J. Am. Chem. Soc.*, 2006, **128**, 13539; T. A. Martinek, A. Hetényi, L. Fülöp, I. M. Mándity, G. K. Tóth, I. Dékány and F. Fülöp, *Angew. Chem., Int. Ed.*, 2006, **45**, 2396.
- 6 A. M. Brückner, P. Chakraborty, S. H. Gellman and U. Diederichsen, *Angew. Chem., Int. Ed.*, 2003, **42**, 4395.
- 7 T. Hirata, F. Fujimura and S. Kimura, *Chem. Commun.*, 2007, 1023.
- 8 For reviews on conformationally constrained amino acids and peptides including cyclobutane derivatives, see: R. M. Ortuño, A. G. Mogliani and G. Y. Moltrasio, *Curr. Org. Chem.*, 2005, **9**, 237; R. M. Ortuño, in *Enantioselective Synthesis of  $\beta$ -Amino Acids*, Second Edition, ed. E. Juaristi and V. A. Soloshonok, John Wiley and Sons, New Jersey, 2005, pp. 117–137.
- 9 M. Martín-Vilà, E. Muray, G. P. Aguado, Á. Álvarez-Larena, V. Branchadell, C. Minguillón, E. Giralt and R. M. Ortuño, *Tetrahedron: Asymmetry*, 2000, **11**, 3569.
- 10 S. Izquierdo, M. J. Kogan, T. Parella, A. G. Mogliani, V. Branchadell, E. Giralt and R. M. Ortuño, *J. Org. Chem.*, 2004, **69**, 5093.
- 11 E. Torres, C. Acosta-Silva, F. Rúa, Á. Álvarez-Larena, T. Parella, V. Branchadell and R. M. Ortuño, *Tetrahedron*, 2009, **65**, 5669.

- 12 S. Izquierdo, F. Rúa, A. Sbai, T. Parella, Á. Álvarez-Larena, V. Branchadell and R. M. Ortuño, *J. Org. Chem.*, 2005, **70**, 7963.
- 13 E. Torres, E. Gorrea, E. Da Silva, P. Nolis, V. Branchadell and R. M. Ortuño, *Org. Lett.*, 2009, **11**, 2301.
- 14 F. Rúa, S. Boussert, T. Parella, I. Diez-Pérez, V. Branchadell, E. Giralt and R. M. Ortuño, *Org. Lett.*, 2007, **9**, 3643.
- 15 D. Fernández, E. Torres, F. X. Avilés, R. M. Ortuño and J. Vendrell, *Bioorg. Med. Chem.*, 2009, **17**, 3824.
- 16 C. Fernandes, C. Gauzy, Y. Yang, O. Roy, E. Pereira, S. Faure and D. J. Aitken, *Synthesis*, 2007, 2222.
- 17 N. Gauvry, C. Comoy, C. Lescop and F. Huet, *Synthesis*, 1999, 574.
- 18 X. Gu, S. R. Xian, J. Bolte, D. J. Aitken and T. Gefflaut, *Tetrahedron Lett.*, 2006, **47**, 193.
- 19 D. C. Owsley and J. J. Bloomfield, *J. Org. Chem.*, 1971, **36**, 3768.
- 20 K. Pearson, *Philos. Mag.*, 1901, **2**, 559; J. Shlens, *A Tutorial on Principal Component Analysis*, 2005, Systems Neurobiology Laboratory, Salk Institute for Biological Studies, La Jolla, CA 92037 and Institute for Nonlinear Science, University of California, San Diego La Jolla, CA 92093-0402. <http://www.sn.l.salk.edu/~shlens/notes.html>; I. T. Jolliffe, *Principal Component Analysis, Series: Springer Series in Statistics*, 2nd edn Springer, NY, XXIX, 2002, pp. 487.
- 21 W. F. van Gunsteren, H. J. C. Berendsen and J. A. C. Rullmann, *Mol. Phys.*, 1981, **44**, 69; W. F. van Gunsteren and H. J. C. Berendsen, *Mol. Phys.*, 1982, **45**, 637.
- 22 For some selected references, see: K. Wang, X. Yan, Y. Cui, Q. He and J. Li, *Bioconjugate Chem.*, 2007, **18**, 1735; X. Yan, Q. He, K. Wang, L. Duan, Y. Cui and J. Li, *Angew. Chem., Int. Ed.*, 2007, **46**, 2431; X. Yan, Y. Cui, Q. He, K. Wang, J. Li, W. Mu, B. Wang and Z. Ou-yang, *Chem.–Eur. J.*, 2008, **14**, 5974; S. Ghosh, M. Reches, E. Gazit and S. Verma, *Angew. Chem., Int. Ed.*, 2007, **46**, 2002; S. Ghosh, S. K. Singh and S. Verma, *Chem. Commun.*, 2007, 2296; S. Ghosh and S. Verma, *Chem.–Eur. J.*, 2008, **14**, 1415.
- 23 D. A. Pearlman, D. A. Case, J. W. Caldwell, W. S. Ross, T. E. Cheatham III, S. DeBolt, D. Ferguson, G. Seibel and P. A. Kollman, *Comp. Phys. Commun.*, 1995, **91**, 1; D. A. Case, D. A. Pearlman, J. W. Caldwell, T. E. Cheatham III, J. Wang, W. S. Ross, C. L. Simmerling, T. A. Darden, K. M. Merz, R. V. Stanton, A. L. Cheng, J. J. Vincent, M. Crowley, V. Tsui, H. Gohlke, R. J. Radmer, Y. Duan, J. Pitera, I. Massova, G. L. Seibel, U. C. Singh, P. K. Weiner and P. A. Kollman, 2002, *AMBER 7*, University of California, San Francisco.
- 24 J. Wang, P. Cieplak and P. A. Kollman, *J. Comput. Chem.*, 2000, **21**, 1049.
- 25 *MacroModel, version 9.0*, Schrödinger, LLC, New York, NY, 2005.
- 26 G. W. Trucks, H. B. Schlegel, G. E. Scuseria, M. A. Robb, J. R. Cheeseman, V. G. Zakrzewski, J. A. Montgomery, Jr., R. E. Stratmann, J. C. Burant, S. Dapprich, J. M. Millam, A. D. Daniels, K. N. Kudin, M. C. Strain, O. Farkas, J. Tomasi, V. Barone, M. Cossi, R. Cammi, B. Mennucci, C. Pomelli, C. Adamo, S. Clifford, J. Ochterski, G. A. Petersson, P. Y. Ayala, Q. Cui, K. Morokuma, P. Salvador, J. J. Dannenberg, D. K. Malick, A. D. Rabuck, K. Raghavachari, J. B. Foresman, J. Cioslowski, J. V. Ortiz, A. G. Baboul, B. B. Stefanov, G. Liu, A. Liashenko, P. Piskorz, I. Komaromi, R. Gomperts, R. L. Martin, D. J. Fox, T. Keith, M. A. Al-Laham, C. Y. Peng, A. Nanayakkara, M. Challacombe, P. M. W. Gill, B. Johnson, W. Chen, M. W. Wong, J. L. Andres, C. Gonzalez, M. Head-Gordon, E. S. Replogle and J. A. Pople, *Gaussian 98, Revision A.11.*, M. J. Frisch, Gaussian, Inc., Pittsburgh PA, 2001.
- 27 S. Kirkpatrick, C. D. Gelatt and M. P. Vecchi, *Science*, 1983, **220**, 671.
- 28 H. J. C. Berendsen, J. P. M. Postma, W. F. van Gunsteren, A. DiNola and J. R. Haak, *J. Chem. Phys.*, 1984, **81**, 3684.
- 29 J. P. Ryckaert, G. Ciccotti and H. J. C. Berendsen, *J. Comput. Phys.*, 1977, **23**, 327; J. P. Ryckaert, *Mol. Phys.*, 1985, **55**, 549.
- 30 J. A. Snyman, *Practical Mathematical Optimization: An Introduction to Basic Optimization Theory and Classical and New Gradient-Based Algorithms*, Springer Publishing, Heidelberg, 2005.
- 31 M. R. Hestenes and E. Stiefel, *J. Res. Nat. Bur. Stand.*, 1952, **49**, 409; E. Polak and G. Ribière, *Rev. Fr. Inform. Rech. O.*, 1969, **16**, 35; R. Fletcher and C. M. Reeves, *Comput. J.*, 1964, **7**, 149.